Al-Salam Journal for Engineering and Technology
Journal Homepage: http://journal.alsalam.edu.iq/index.php/ajest
e-ISSN: 2790-4822p-ISSN: 2958-0862

Decomposing Method for Space-Time Fractional Order PDEs

Ahmed Shukur [1], Ahmed Shawki Jaber[2], Mohammed RASHEED[1, 3]*, Tarek Saidani[4]

[1]Applied Sciences Department, University of Technology - Iraq, Baghdad, Iraq.
[2]Mathematics Science Department, College of Science, Mustansiriyah University, Baghdad, Iraq.
[3]MOLTECH Anjou, Universite d'Angers/UMR CNRS 6200, 2, Bd Lavoisier, 49045 Angers, France.
[4]Department of Physics, Akli Mohaned Oulhadj University of Bouira, Bouira, 10000, Algeria.

*Corresponding Author: Mohammed RASHEED

DOI: https://doi.org/10.55145/ajest.2024.03.02.01
Received Febuary 2024; Accepted April 2024; Available online online May 2024

ABSTRACT: Numerical solutions to integer-order differential equations frequently employ decomposition as one of many methods. This paper provides a generalization of integer-order differential equations into fractional order, which is more general, as well as generalizing the decomposing method into the fractional case and then applying it to solve differential equations of fractional order in both space and time. A fractional calculus's theorems and properties to generalize both differential equations and the decomposition method have been utilized. This method to solve different fractional time and space partial differential equations, demonstrating its ability and applicability to various problems have been applied. The method to various cases to highlight its strengths has been used. The graphs and tables of results obtained using Matlab programs have been presented and discussed.

Keywords: Decomposition technique, space-time, fractional equations

1. INTRODUCTION

Changing in the natural and the scientific phenomenon need solutions, the field of fractional calculus gives these problems, the best solutions, so the work in this field become better than integer calculus. One can see the fact, now almost, researchers write in this field and they solve many different problems in many sciences using different methods. In [1] Kudryashov technique is utilized for the resolution of nonlinear space-time fractional partial differential equations. The linear fractional partial differential equations were solved using the local fractional Sum udu decomposition technique in [2-3]. The authors use an approximation technique to solve differential equations including fractional order delay in [4]. The use of the Decomposition Method and its implications in the resolution of Linear and Nonlinear Schrödinger Equations is explored in [5]. The Delay-Decomposing Approaches to Absolute Stability Criteria for Neutral-Type Lur'e Systems were examined in [6]. The optimum homotopy asymptotic approach is used in [7] to solve first-order nonlinear fuzzy differential equations. The objective of this study is to provide an approximate solution for a first-order nonlinear fuzzy initial value problem that involves two distinct fuzzy functions [8]. By using the Decomposition transform technique, Fractional Differential Equations are solved in [9]. The solution to the system of Volterra-Fredholm Integro-Differential Equations is obtained using numerical methods in [10]. Moreover one can see the fractional field almost, in all sciences because it gives the right Explanation for the scientific phenomenon. The main work in this paper is generalizing of decomposition method and showing the powerful and utilizing to solve fractional order partial differential equations, solving some of them here that can write the general form of orders bounded by two by the following:

*Corresponding author: rasheed.mohammed40@yahoo.com

$$\frac{\partial^{\upsilon}\phi(x,\tau)}{\partial x^{\upsilon}} = a\frac{\partial^{\sigma}\phi(x,\tau)}{\partial \tau^{\sigma}} + b\frac{\partial^{\rho}\phi(x,\tau)}{\partial \tau^{\rho}} + c\phi(x,\tau) + \omega(x,\tau) \quad (1)$$

where $0 < x < L; \tau > 0; 1 < (\upsilon;\sigma) \leq 2; 0 < \rho \leq 1$; a, b and c are constants, $\omega(x,\tau)$ is a given function, subject to initial and boundary conditions as

Initial conditions (I.C 1) $\phi(x,0) = \lambda_1(x)$ and (I.C 2) $\phi_x(x,\tau)_{\tau=0} = \lambda_2(x)$ (2)

(B.C 1) $\phi(0,\tau) = \theta_1(\tau)$ and (B.C 2) $\phi(L,\tau) = \theta_2(\tau)$ (3)

If (ω(x,τ)=0), the equation will be a linear homogeneous Space-Time fractional partial differential equation. Conversely, if (a = c = 0), the equation will result in the Space-Time Like-heat equations. In the scenario when b = c = 0, the resulting equation may be expressed as the Space-Time Like-Wave equations.

The aim of this study is to generalize integer-order differential equations into fractional order and extend the decomposing method to the fractional case. This is achieved by utilizing fractional calculus theorems and properties to solve fractional time and space partial differential equations. The study demonstrates the method's ability and applicability to various problems by applying it to different cases and presenting the results using Matlab programs.

2. Definitions and Theorems [11- 21]

Some definitions given as a base in this work

2.1 Riemann integration (RFI) of order (γ) OR $\left({}_cJ_\tau^\gamma OR {}_cD_\tau^{-\gamma}\right)$ [22-25]

The formula for fractional order integration, as shown below in modern notation, was derived by Riemann via the use of an extension of the Taylor series

$$J^\gamma f(\tau) = D^{-\gamma} f(\tau) = \frac{1}{\Gamma(\gamma)}\int_c^\tau (\tau - s)^{\gamma-1} f(s)ds + \psi(s) \quad (4)$$

Riemann introduced an arbitrary (complementary) function ψ(s) because he did not fix the lower bound of integration c, a disadvantage that cannot be removed in the framework of his approach.

2.2 Riemann-Liouvill Fractional Derivative (RFD) of order $(\boldsymbol{\gamma})$, $\mathbf{OR}$ ${}_c^R\mathbf{D}_\tau^\gamma \mathbf{f}(\boldsymbol{\tau})$, given as:

$${}_c^R D_\tau^\gamma f(\tau) = \frac{1}{\Gamma(n-\gamma)}\left(\frac{d}{d\tau}\right)^n \int_c^\tau \frac{f(s)ds}{(\tau-s)^{\gamma-n+1}} \quad (5)$$

where $n-1 \leq \gamma < n; n = \lceil\gamma\rceil$

2.3 Caputo Fractional Derivative (CFD) of order (γ), or ${}_a^C\mathbf{D}_\tau^\gamma \mathbf{f}(\boldsymbol{\tau})$, where $\mathbf{n-1 < \gamma < n}$,

$${}_a^C D_\tau^\gamma f(\tau) = J_\tau^{n-\gamma} D_\tau^n f(\tau) = \begin{cases} \left[\frac{1}{\Gamma(n-\gamma)}\int_c^\tau (\tau-s)^{n-\gamma-1}\left(\frac{d}{ds}\right)^n f(s)ds\right]; n-1 < \gamma < n \\ \left(\frac{d}{d\tau}\right)^n f(\tau) \qquad\qquad \gamma = n \end{cases} \quad (6)$$

2.4 Properties (Riemann and Caputo) Fractional Derivatives and Riemann Integral

i- $(\gamma \text{ and } \upsilon) \epsilon \mathbb{R}; 0 \leq (\gamma \text{ and } \upsilon)$ then $J_\tau^\gamma J_\tau^\upsilon = J_\tau^\upsilon J_\tau^\gamma = J_\tau^{\gamma+\upsilon}$ (7)

ii- For $0 \leq \gamma$; $-1 < \sigma$ then $J_\tau^\gamma \tau^\sigma = \frac{\Gamma(\sigma+1)}{\Gamma(1+\sigma-\gamma)}\tau^{\sigma-\gamma}$ (8)

From definitions and Properties if $\gamma \to (n-1)$ then

iii- ${}_a^C D_\tau^\gamma f(\tau) \to J_\tau^{n-(n-1)} D_\tau^n f(\tau) = J_\tau^{+1} D_\tau^n f(\tau) = D_\tau^{n-2} f(0) - D_\tau^{n-1} f(0)$ (9)

iv- $$\begin{cases} J_\tau^\gamma \ {}_a^C D_\tau^\gamma f(\tau) = f(\tau) \\ J_\tau^\gamma \ {}_a^C D_\tau^\gamma f(\tau) = f(\tau) - \sum_{k=0}^{n-1} j^{(k)}(0^+)\frac{\tau^k}{k!} \end{cases} \quad ; \ \tau > 0 \quad (10)$$

Note 1: Is Caputo's fractional derivative superior to other formulae for the fractional differential equation (FDE)? The rationale for the use of the Caputo definition is in the need to delineate supplementary criteria in order to provide a distinct solution. The supplementary conditions mentioned are only conventional conditions, similar to those found in classical differential equations, and so are easily recognizable to humans. In contrast, the Riemann-Liouville fractional derivative definition includes specific fractional derivatives (and/or integrals) of the unknown solution at the beginning point x = 0, which are functions of x. The beginning circumstances lack physical characteristics, and the method for measuring these quantities in tests is unclear, making it difficult to allocate them accurately in an analysis [26-30].

Note 2: In this note, some of the fractional derivatives can be written by using the linearity and properties of fractional derivatives with the help of expansion series of the power for some functions as the following: let, we can write a function f(x) by expansion formas:

$f(\tau) = \sum_{k=-\infty}^{+\infty} a_k \frac{\tau^k}{k!}$ where a_k are constants, then fractional derivatives can be written as:

$$ {}_{a}^{C}D_{\tau}^{\gamma} f(\tau) = \sum_{k=-\infty}^{+\infty} a_k \frac{(k!)\,\tau^{k-\gamma)}}{(k!)\Gamma(1+k-\gamma)} \tag{11} $$

If $f(\tau) = e^{a\tau}$ then ${}_{a}^{C}D_{\tau}^{\gamma} f(\tau) = a^{\gamma} e^{a\tau}$ where $a \in \mathbb{R}$ (12)

$$ \text{If } f(\tau) = \sin(\tau) \text{ or } f(\tau) = \cos(\tau), \text{ then } {}_{a}^{C}D_{\tau}^{\gamma} f(\tau) = \begin{cases} \sin\left(\tau + \frac{\pi\gamma}{2}\right) \\ \cos\left(\tau + \frac{\pi\gamma}{2}\right) \end{cases} \tag{13} $$

$$ \text{If } f(\tau) = e^{\tau}\sin(\tau) \text{ or } f(\tau) = e^{\tau}\cos(\tau), \text{ then } {}_{a}^{C}D_{\tau}^{\gamma} f(\tau) = \begin{cases} 2^{\tau/2} e^{\tau} \sin\left(\tau + \frac{\pi\gamma}{4}\right) \\ 2^{\tau/2} e^{\tau} \cos\left(\tau + \frac{\pi\gamma}{4}\right) \end{cases} \tag{14} $$

3. Decomposing method

The proposed approach involves directly addressing the equations and advancing them without using linearization, perturbation, or other constraining assumptions that might potentially alter the physical characteristics of the model being examined. Furthermore, the approach involves the decomposition of the unidentified function into an unlimited number of components, which are specified by creating a series. The determination of these components is an iterative process.

3.1 Algorithm of decomposition method

In this section, the general steps will be given as an algorithm to help us solve fractional differential equations; Consider the boundary fractional order Like-Wave equation in the form:

$$ \frac{\partial^{\sigma}\phi(x,\tau)}{\partial\tau^{\sigma}} = \frac{\partial^{\upsilon}\phi(x,\tau)}{\partial x^{\upsilon}} + \omega(x,\tau) \text{ ; where } 0 < x < L;\ \tau \geq 0;\ \sigma \leq 2 . \tag{15} $$

where $\omega(x,\tau)$ is given function, subject to the boundary and initial conditions respectively:

$$ \text{(I.C 1) } \phi(x,0) = \lambda_1(x) \text{ and (I.C 2) } \phi_x(x,\tau)_{\tau=0} = \lambda_2(x) \tag{16} $$

(B.C 1) $\phi(0,\tau) = \theta_1(\tau)$ and (B.C 2) $\phi(L,\tau) = \theta_2(\tau)$

First, Rewrite equation (9) using operator forms as, $D_{\tau}^{\sigma}\phi(x,\tau) = D_{x}^{\upsilon}\phi(x,\tau) + \omega(x,\tau)$ (17)

Second, Choose for what variable which is solving for it (let it τ),

Third, take J_{τ}^{σ} an inverse operator of D_{τ}^{σ} for both sides of the equation in (second),

So that equation will be $J_{\tau}^{\sigma}\, D_{\tau}^{\sigma}\phi(x,\tau) = J_{\tau}^{\sigma}\, D_{x}^{\upsilon}\phi(x,\tau) + J_{\tau}^{\sigma}\, \omega(x,\tau)$, (18)

Using properties in (3, iv),

$$ \phi(x,\tau) = \sum_{k=0}^{n-1} \phi^{(k)}(x,0^{+}) \frac{\tau^k}{k!} + J_{\tau}^{\sigma}\, \omega(x,\tau) + J_{\tau}^{\sigma}\, D_{x}^{\upsilon}\phi(x,\tau) \text{ , } n-1 < \sigma \leq n \tag{19} $$

Fourth, rewrite this solution $\phi(x,\tau)$ by decomposition infinite series as,

$$ \phi(x,\tau) = \sum_{k=0}^{\infty} \phi_k(x,\tau) = (\phi_0, \phi_1, + \cdots + \phi_m + \cdots) \tag{20} $$

$$ \text{then, } \phi(x,\tau) = (\phi_0, \phi_1, + \cdots) = \sum_{k=0}^{n-1} \phi^{(k)}(x,0^{+}) \frac{\tau^k}{k!} + J_{\tau}^{\sigma}\, \omega(x,\tau) + J_{\tau}^{\sigma} \sum_{k=0}^{\infty} D_{x}^{\upsilon}\phi_k \tag{21} $$

Fifth, rewrite the equation in (fourth) as recursive equations:

$$ \begin{cases} \phi_0(x,\tau) = \sum_{k=0}^{n-1} \phi^{(k)}(x,0^{+}) \frac{\tau^k}{k!} + J_{\tau}^{\sigma}\, \omega(x,\tau)\,, & n = \lceil\sigma\rceil \\ \phi_{k+1}(x,\tau) = J_{\tau}^{\sigma} \sum_{k=0}^{\infty} D_{x}^{\upsilon}\phi_k\,, & where \quad k = 0,1,2,3,\ldots \end{cases} \tag{22} $$

Now one can calculate (k^{th})approximation solution by using Eq. (11), where the exact solution will be limited to approximation when k goes to infinite.

4. Numerical Examples

Multiple examples will be resolved to demonstrate the efficacy of this approach.

Example 1

Solve the space-time fraction partial differential like-telegraph equation, respect to initial conditions in the following:

$$\frac{\partial^{\upsilon}\phi(x,\tau)}{\partial x^{\upsilon}} = \frac{\partial^{\sigma}\phi(x,\tau)}{\partial \tau^{\sigma}} + \frac{\partial^{\alpha}\phi(x,\tau)}{\partial \tau^{\alpha}} - \phi(x,\tau), \quad (23)$$

Subject to conditions $\phi(x,\tau)|_{x=0^+} = e^{-\tau}$; $\phi_x(x,\tau)|_{x=0^+} = e^{-\tau}$? (24)

Solution

Using the algorithm above, and the given conditions, one can calculate zero approximation solution as:

$$\phi_0(x,\tau) = \sum_{k=0}^{n-1} \phi_x^{(k)}(x,\tau)|_{x=0^+} \frac{x^k}{k!} = e^{-\tau} + xe^{-\tau} = [1+x]e^{-\tau}, \text{ where n=2,} \quad (25)$$

Take the inverse operator (J_x^{υ}), and using an algorithm to calculate (k^{th}) approximation solution as:

$$\phi_{k+1}(x,\tau) = J_x^{\upsilon}\left[\left(\frac{\partial^{\sigma}}{\partial\tau^{\sigma}} + \frac{\partial^{\alpha}}{\partial\tau^{\alpha}} - 1\right)\phi_k(x,\tau)\right] \qquad k \geq 0, \quad (26)$$

Now, let $(A^{\beta}) = (-1)^{\beta}$, and using properties of fractional integrals and derivatives,

$$\phi_1(x,\tau) = J_x^{\upsilon}\left[\left(\frac{\partial^{\sigma}}{\partial\tau^{\sigma}} + \frac{\partial^{\alpha}}{\partial\tau^{\alpha}} - 1\right)\phi_0(x,\tau)\right] = J_x^{\upsilon}(A^{\sigma} + A^{\alpha} + 1)e^{-\tau}, \quad (27)$$

$$\phi_1(x,\tau) = \left[\frac{x^{\upsilon}}{\Gamma(\upsilon+1)} + \frac{x^{\upsilon+1}}{\Gamma(\upsilon+2)}\right](A^{\sigma} + A^{\alpha} + 1)e^{-\tau}, \quad (28)$$

$$\phi_2(x,\tau) = \left[\frac{x^{2\upsilon}}{\Gamma(2\upsilon+1)} + \frac{x^{2\upsilon+1}}{\Gamma(2\upsilon+2)}\right](A^{\sigma} + A^{\alpha} + 1)^2 e^{-\tau} \quad (29)$$

$$\vdots$$

So that, one can find the (k^{th}) approximation solution as:

$$\phi_k(x,\tau) = \left[\frac{x^{k\upsilon}}{\Gamma(k\upsilon+1)} + \frac{x^{k\upsilon+1}}{\Gamma(k\upsilon+2)}\right](A^{\sigma} + A^{\alpha} + 1)^k; \quad (30)$$

Also limit of this approximation solution gives the exact solution when k goes to infinite as:

$\phi(x,\tau) = \sum_{j=0}^{\infty}\phi_j(x,\tau) = \lim_{k\to\infty}\sum_{j=0}^{k}\phi_j(x,\tau)$; If $\upsilon = \sigma = 2$ and $\alpha = 1$, then limit of infinite sum gives exact solution of the integer order telegraph equation as:

$$\phi(x,\tau) = \lim_{k\to\infty}\sum_{j=0}^{k}\phi_j(x,\tau) = e^{2x}e^{-\tau}. \quad (31)$$

Figure 1 shows the curves of exact solution, where, $\phi(x,\tau) = e^{2x}e^{-\tau}$,at $\upsilon = \sigma = 2$ and $\alpha = 1$, and the approximation solution where, ($k = 7, \upsilon = \sigma = 2$ and $\alpha = 1$).

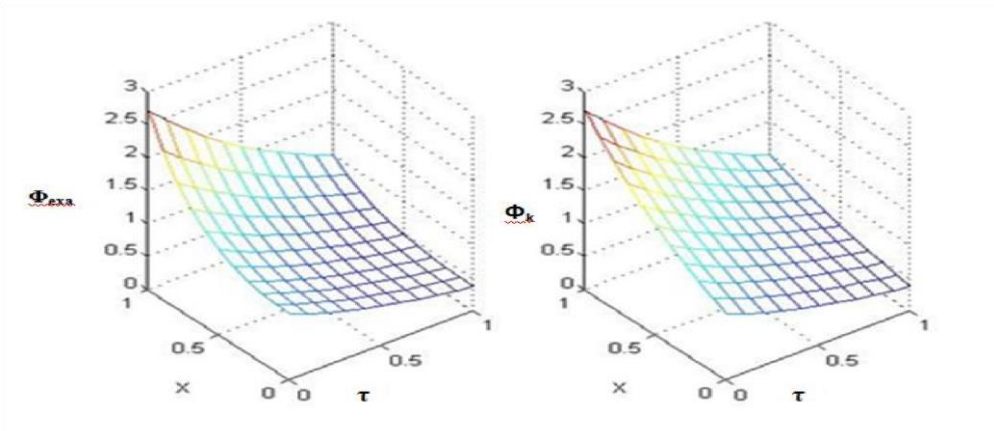

FIGURE 1. - One can see (left-side) graph of exact solution which is given by function ($e^{2x}e^{-\tau}$) is closed with the (right-side) graph of K^th approximation solution which is given by $\phi_k(x,\tau)$, where ($k = 7, \upsilon = \sigma = 2$ and $\alpha = 1$)

Figure 1 displays two graphs side by side.

On the left side, the graph represents the exact solution, given by the function $e^{2x}e^{-\tau}$. This function is plotted against the variables x and τ. The shape of this graph provides insight into the behavior of the exact solution over the specified range of x and τ.

On the right side, the graph illustrates the K[th] approximation solution, denoted as $\phi_k(x, \tau)$, where k=7, ν=σ=2, and α=1. This approximation solution is also plotted against the variables x and τ. The shape and characteristics of this graph depict how well the approximation captures the behavior of the exact solution.

By juxtaposing the exact solution with the K[th] approximation solution, the figure provides a visual comparison, allowing for an assessment of the accuracy of the approximation method in replicating the behavior of the system. This comparison helps to evaluate the effectiveness of the approximation technique in representing the exact solution under the given conditions.

Figure 2 shows the curves of exact solution, where, $\phi(x,\tau) = e^{2x}e^{-\tau}$, at $\upsilon = \sigma = 2$ and $\alpha = 1$,and approximation solutions at 7 terms only, where ($k = 7, \upsilon = 1.5, \sigma = 2$ and $\alpha = 1$.

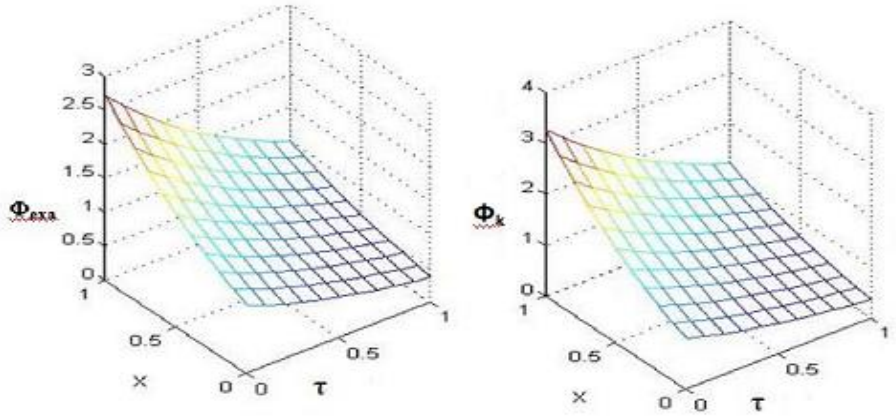

FIGURE 2. - One can see what happen in the (left-side) graph of approximation solution when we change the derivative ($\upsilon = 1.5$) from ($\upsilon = 2$), but in general the approximation solution will be closed with exact when all derivatives go from fractional order to integer

Figure 2 depicts the curves of the exact solution, represented by ϕ(x,τ), and the approximation solutions using only 7 terms.

Specifically, the left side of the graph displays the curves of the exact solution ϕ(x, τ) at ν=σ=2 and α=1. This curve represents the behavior of the exact solution over the specified range of x and τ.

On the right side of the graph, the curves represent the approximation solutions using only 7 terms, where k=7, ν=1.5, σ=2, and α=1. These curves illustrate how well the approximation method captures the behavior of the exact solution with a limited number of terms.

By juxtaposing the curves of the exact solution with those of the approximation solutions, the figure facilitates a visual comparison. This comparison enables an assessment of the accuracy and effectiveness of the approximation technique in replicating the behavior of the exact solution under the specified conditions.

Example 2

Solve like-wave fractional order partial differential equations,

$$\frac{\partial^{\sigma}\phi(x,\tau)}{\partial\tau^{\sigma}} = \frac{\partial^{\upsilon}\phi(x,\tau)}{\partial x^{\upsilon}} \quad \text{where, } 1 < (\upsilon,\ \sigma) \leq 2, 0 < x < L, \tau > 0. \tag{32}$$

Concerning conditions as: $\phi(x,\tau)|_{\tau=0^+} = \cos(x)\,;\ \phi_{\tau}(x,\tau)|_{\tau=0^+} = \cos(x).$ (33)

Solution

Using initial conditions to find zero approximation solution as:

$$\phi_0(x,\tau) = [\cos(x) + \tau\cos(x)] = (1+\tau)\cos(x); \tag{34}$$

Also the (kth) approximation given:

$$\phi_{k+1}(x,\tau) = J_{\tau}^{\sigma}[D_x^{\upsilon}\phi_k(x,\tau)] \text{ k= 0, 1, 2, 3, … etc.;} \tag{35}$$

one can use that to find: $$\phi_1(x,\tau) = J_{\tau}^{\sigma}[D_x^{\upsilon}\phi_0(x,\tau)] = J_{\tau}^{\sigma}(1+\tau)\left[\cos(x+\tfrac{\upsilon\pi}{2})\right], \tag{36}$$

$$\phi_1(x,\tau) = \left[\frac{\tau^{\sigma}}{\Gamma(\sigma+1)} + \frac{\tau^{\sigma+1}}{\Gamma(\sigma+2)}\right]\left[\cos(x+\frac{\upsilon\pi}{2})\right], \quad (37)$$

by the same way, one can find:

$$\phi_2(x,\tau) = \left[\frac{\tau^{2\sigma}}{\Gamma(2\sigma+1)} + \frac{\tau^{2\sigma+1}}{\Gamma(2\sigma+2)}\right]\left[\cos(x+\frac{2\upsilon\pi}{2})\right], \text{ so on} \quad (38)$$

$$\vdots$$

$$\phi_k(x,\tau) = \left[\frac{\tau^{k\sigma}}{\Gamma(k\sigma+1)} + \frac{\tau^{k\sigma+1}}{\Gamma(k\sigma+2)}\right]\left[\cos(x+\frac{k\upsilon\pi}{2})\right] \quad (39)$$

This formula gives the approximation solutions for $k > 1$, also one can find the exact solution when k goes to infinity as:

$$\phi(x,\tau) = \sum_{j=0}^{\infty}\phi_j(x,\tau) \;\; OR \;\; \lim_{k\to\infty}\sum_{j=0}^{k}\phi_j(x,\tau)\,; \quad (40)$$

where this means:

$$\phi(x,\tau) = \sum_{k=0}^{\infty}\left[\frac{\tau^{k\sigma}}{\Gamma(k\sigma+1)} + \frac{\tau^{k\sigma+1}}{\Gamma(k\sigma+2)}\right]\left[\cos(x+\frac{k\upsilon\pi}{2})\right], \text{ then at } (\upsilon = \;\; \sigma = 2) \quad (41)$$

solution will

$$\phi(x,\tau) = \sum_{k=0}^{\infty}(-1)^k\left[\frac{\tau^{k\sigma}}{\Gamma(k\sigma+1)} + \frac{\tau^{k\sigma+1}}{\Gamma(k\sigma+2)}\right]\left[\cos(x+\frac{k\upsilon\pi}{2})\right] = \cos(x)\,[\cos(\tau)+\sin(\tau)] \quad (42)$$

This solution closed with the exact solution of the wave partial differential equation of integer order.

Figure 3 presents the curves of exact solution ($\phi(x,\tau)=\cos(x)\,[\cos(\tau)+\sin(\tau)]$), and the approxim- ation solutions $\phi(x,\tau) = \sum_{k=0}^{10}\left[\frac{\tau^{k\sigma}}{\Gamma(k\sigma+1)} + \frac{\tau^{k\sigma+1}}{\Gamma(k\sigma+2)}\right]\left[\cos(x+\frac{k\upsilon\pi}{2})\right]$, where x =(0:0.1:1), with fixed $\tau = 0.4$, also taken $\phi_k(x,\tau)\; at\; different\; \upsilon\; and\; \sigma$ (43)

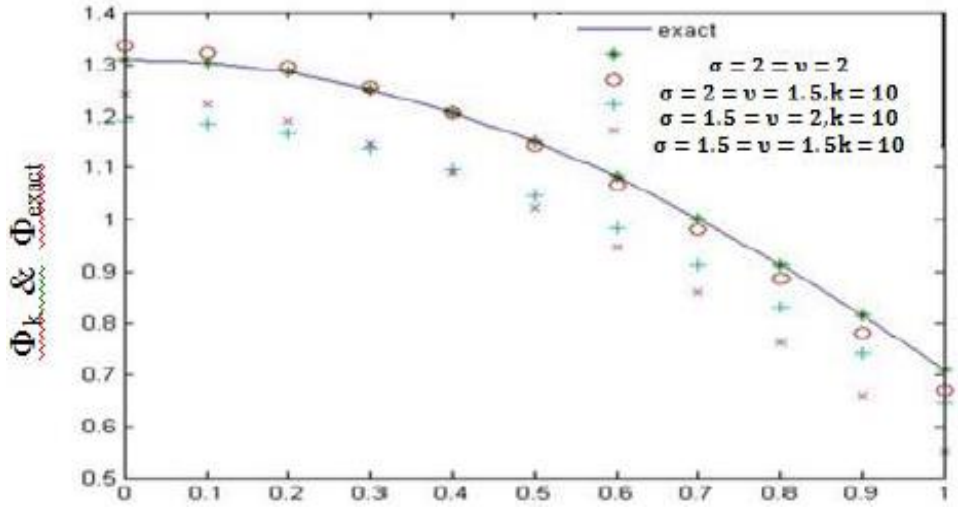

FIGURE 3. - One can see the four curves (*, +, o, and *) of approximation solutions, go to close with exact solution curve (_____) when the derivatives go from fractional order to integer order at the Kth solution

Figure 3 displays the comparison between the exact solution and the approximation solutions for Example 2.

The exact solution, represented by the curve labeled "_____", is given by $\phi(x,\tau)=\cos(x)[\cos(\tau)+\sin(\tau)]$. This function is plotted against the variables x and τ.

The approximation solutions, represented by the curves labeled "", "+", "o", and "*", are computed using the formula Eq. 34. These curves are plotted for x values ranging from 0 to 1 with increments of 0.1, and with a fixed τ value of 0.4. Additionally, the approximation solutions are evaluated at different values of ν and σ.

By comparing the curves of the exact solution with those of the approximation solutions, the figure illustrates how closely the approximation solutions approach the behavior of the exact solution. As the derivatives transition from fractional order to integer order, the approximation solutions converge towards the exact solution. This convergence is visually depicted by the approximation solution curves moving closer to the exact solution curve as the fractional orders approach integer values. The figure demonstrates the effectiveness of the approximation method in capturing the dynamics of the system, particularly as the fractional orders approach integer values.

Figure 4: presents the curve of the exact solution and the approximate solution, where $k = 10, \upsilon = \sigma = 1.8$.

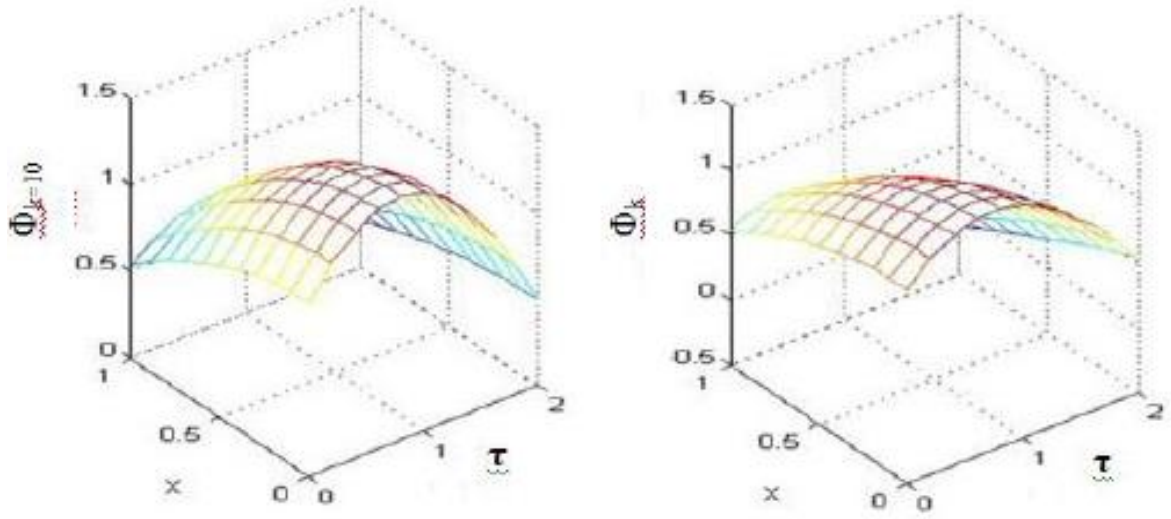

FIGURE 4. - This drawing shows us how the drawing of the approximate solution on the right side is close to the same shape as the real solution, and that the difference is due to the difference in the partial derivatives in each of ($\upsilon = \sigma = 1.8$)

Figure 4 illustrates the comparison between the exact solution and the approximate solution for a specific scenario characterized by k=10 and ν=σ=1.8.

On the left side of the graph, the curve represents the exact solution of the problem. This solution, likely plotted against variables such as x and τ, accurately describes the behavior of the system according to the given fractional partial differential equation.

On the right side of the graph, the curve depicts the approximate solution derived using the approximation method. This solution is also plotted against the same variables as the exact solution.

The accompanying explanation suggests that the approximate solution closely resembles the shape of the exact solution. However, there are slight differences between the two curves, attributed to variations in the partial derivatives involved in computing the solutions. Specifically, these differences arise from the use of fractional orders (ν=σ=1.8) in the approximation, in contrast to the integer orders in the exact solution. The figure demonstrates the effectiveness of the approximation method in capturing the behavior of the system. The close similarity between the approximate and exact solutions indicates that the approximation method yields results that closely resemble the true dynamics of the system, albeit with slight differences due to the use of fractional orders.

Example 3

Solve the general fractional space-time Like-heat homogeneous partial differential equation, $\frac{\partial^{\sigma}\phi(x,\tau)}{\partial\tau^{\sigma}} = \frac{\partial^{\upsilon}\phi(x,\tau)}{\partial x^{\upsilon}}, where\ 0 < \sigma \leq 1 < \nu \leq 2, 0 < x < L, \tau > 0$, subject to condition, $\phi(x,\tau)|_{\tau=0^+} = \sin x$? (44)

Solution

By using the given condition and the algorithm of this method, one can find the zero solution as: $\phi_0(x,\tau) = \sin x$, then (k^{th}) approximation solution given as:

$\phi_{k+1}(x,\tau) = j_{\tau}^{\sigma}[D_x^{\upsilon}\phi_k(x,\tau)]$, where k = 0, 1, 2,…, (45)

now use these equations to find:

$$\phi_1(x,\tau) = j_{\tau}^{\sigma}[D_x^{\upsilon}\phi_0(x,\tau)] = j_{\tau}^{\sigma}[D_x^{\upsilon}\sin x] = \frac{\tau^{\sigma}}{\Gamma(\sigma+1)}\left[\sin(x+\frac{\upsilon\pi}{2})\right], \quad (46)$$

$$\phi_2(x,\tau) = j_{\tau}^{\sigma}[D_x^{\upsilon}\phi_0(x,\tau)] = j_{\tau}^{\sigma}\frac{\tau^{\sigma}}{\Gamma(\sigma+1)}\left[\sin(x+\frac{\upsilon\pi}{2})\right] = \frac{\tau^{2\sigma}}{\Gamma(2\sigma+1)}\left[\sin(x+\frac{2\upsilon\pi}{2})\right] \quad (47)$$

⋮

So, (k^{th}) solution will be: $\phi_k(x,\tau) = \frac{\tau^{k\sigma}}{\Gamma(k\sigma+1)}\left[\sin(x+\frac{k\upsilon\pi}{2})\right], where\ k = 0,1,\ldots$ (48)

Also, the exact solution will be a limit of the (k^{th}) solution, when k goes to infinite,

$$\phi(x,\tau) = \lim_{k\to\infty} \sum_{j=0}^{k} \phi_j(x,\tau) = \lim_{k\to\infty} \sum_{j=0}^{k} \frac{\tau^{j\sigma}}{\Gamma(j\sigma+1)} \left[\sin(x + \frac{j\nu\pi}{2})\right], \quad (49)$$

$$\phi(x,\tau) = \sin x \lim_{k\to\infty} \sum_{j=0}^{k} (-1)^j \frac{\tau^j}{\Gamma(j+1)} = e^{-\tau} \sin x, \quad (50)$$

Then this closed with the solution of the same equation in integer derivatives $(\sigma = 1;\ \nu = 2)$.

Figure 5 shows the exact solution and the estimated solutions for various values of (σ, ν) with k=10 terms, one can see how the figure of approximation moves to close with the exact curve when the values of fractional derivative closed with integer values.

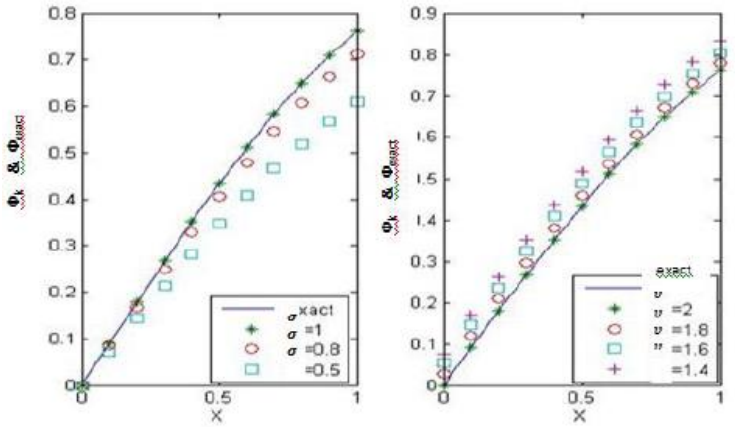

FIGURE 5. - Here the left drawing shows us how the approximate solution curve approaches the exact, when the value of the fractional order derivative (σ) increases to integer derivative, with fixed (ν=2), also, the right-side drawing shows us how the approximate solution approaches the exact, when the fractional derivative (ν) go to integer derivative (ν=2), with fixed (σ=1). Both of them show us the approximate solution curve conforms to the exact one when the fractional derivatives reach the integer derivatives (σ=1, ν=2)

Figure 5 illustrates the comparison between the exact solution and the estimated solutions for Example 3, considering various values of σ and ν with k=10 terms.

The left drawing in Figure 5 demonstrates how the approximate solution curve approaches the exact solution curve as the value of the fractional order derivative (σ) increases towards an integer derivative, with a fixed ν=2. This behavior is depicted by plotting the approximate solutions for different values of σσ against the exact solution. As σ approaches 1 (an integer value), the approximate solution curve gradually becomes closer to the exact solution curve.

Similarly, the right-side drawing in Figure 5 illustrates how the approximate solution curve approaches the exact solution curve as the fractional derivative (ν) approaches an integer derivative (ν=2), with a fixed σ=1. Again, the behavior is depicted by plotting the approximate solutions for different values of ν against the exact solution. As ν approaches 2 (an integer value), the approximate solution curve becomes more similar to the exact solution curve.

Overall, both drawings in Figure 5 highlight how the approximate solution curve converges towards the exact solution curve as the fractional derivatives (σ and ν) approach integer values. This convergence indicates the effectiveness of the approximation method, particularly in capturing the behavior of the system accurately when the fractional derivatives closely resemble integer derivatives.

Table 1 demonstrates the juxtaposition of exact and approximate solutions across many values of (σ, ν) and (x=0:0.1:1), fixed τ = 0.5. One can see the errors between exact and approximation solutions, these errors become small when fractional derivatives equal integers.

Table 1. – The exact and approximate solutions for example 3

τ	x	Φ_{exact}	$\Phi_{\nu=2}^{\sigma=1}$	$\Phi_{\nu=1.5}^{\sigma=1}$	$\Phi_{\nu=2}^{\sigma=0.7}$
Fixed τ=0.5	0.000	0.000	0.000	0.0341	0.000
	0.1000	0.0950	0.0950	0.1303	0.0875
	0.2000	0.1890	0.1890	0.2251	0.1741
	0.3000	0.2811	0.2811	0.3177	0.2589
	0.4000	0.3704	0.3704	0.4071	0.3412
	0.5000	0.4560	0.4560	0.4924	0.4201
	0.6000	0.5371	0.5371	0.5728	0.4947

	0.7000	0.6128	0.6128	0.6475	0.5644
	0.8000	0.6824	0.6824	0.7158	0.6285
	0.9000	0.7451	0.7451	0.7769	0.6863
	1.000	0.8004	0.8004	0.8302	0.7373

From Table 1 the exact and approximate solutions for example 3, with a fixed value of $\tau = 0.5$ and varying values of x in the range from 0 to 1 with increments of 0.1 has been presented.
In the table, the first column represents the values of x, while the subsequent columns display the exact solution, the approximate solution, and the errors between them. The errors are computed as the absolute difference between the exact and approximate solutions.

The table demonstrates how the errors between the exact and approximate solutions change as the fractional derivatives approach integer values. Specifically, it notes that the errors become smaller when the fractional derivatives approach integers. This observation suggests that the accuracy of the approximate solutions improves as the fractional derivatives become closer to integer values.

The table provides a quantitative comparison between the exact and approximate solutions, highlighting the efficacy of the approximation method in capturing the behavior of the system, particularly as the fractional derivatives converge towards integer values.

Example 4

Solve the following linear inhomogeneous fractional order space-time partial differential equation:

$$ {}_a^C D_\tau^{0.5}\phi(x,\tau) = {}_a^C D_x^{1.5}\phi(x,\tau) + \omega(x,\tau), \; 0 < x < 1, \tau \geq 0 \quad (51)$$

Subject to boundary and initial condition respectively

$$\text{B.C } \phi(0,\tau) = 0, \phi(1,\tau) = e^{-\tau} where \tau \geq 0, \; \text{I.C } \phi(x,0) = x^2 \; where \; 0 < x < 1, \quad (52)$$

also the given function is:

$$\omega(x,\tau) = \frac{1}{\Gamma(1.5)} x^2 \, J_\tau^{0.5} \, e^{-\tau} - \frac{\Gamma(3)}{\Gamma(1.5)} x^{0.5} \; e^{-\tau} \quad (53)$$

Solution

This equation has been solved for τ unknown variable

$$\phi_0(x,\tau) = \phi(x,0) + J_\tau^{0.5}\omega(x,\tau), \text{ and } \phi_{k+1}(x,\tau) = J_\tau^{0.5} \, {}_a^C D_x^{1.5}\phi(x,\tau), \text{ for } \tau \geq 0, \quad (54)$$

Then

$$\phi_0(x,\tau) = x^2 + J_\tau^{0.5}[(x^2 D_x^{1.5} e^{-\tau}) - (\frac{\Gamma(2+1)}{\Gamma(2-1.5+1)} x^{(2-1.5)} e^{-\tau})] \quad (55)$$

$$\phi_0(x,\tau) = x^2 + x^2(e^{-\tau} - 1) - J_\tau^{0.5}[\frac{\Gamma(2+1)}{\Gamma(2-1.5+1)} x^{(2-1.5)} e^{-\tau}], \quad (56)$$

$$\phi_0(x,\tau) = x^2 e^{-\tau} + -J_\tau^{0.5}[\frac{\Gamma(3)}{\Gamma(3-1.5)} x^{(0.5)} e^{-\tau}], \quad (57)$$

$$\phi_1(x,\tau) = J_\tau^{0.5} D_x^{1.5}\phi_0(x,\tau) = J_\tau^{0.5}[\frac{\Gamma(3)}{\Gamma(3-1.5)} x^{(0.5)} e^{-\tau}] - J_\tau^{0.5}[\frac{\Gamma(3)}{\Gamma(3-3)} x^{(2-3)} e^{-\tau}] \quad (58)$$

One of the powerful features of this method appears in this example: when we solving inhomogeneous fractional order partial differential equations, we obtain two similar terms that are equal in two successive steps but with different signs. Therefore, when collecting the terms to obtain the final solution, these terms will disappear and we obtain the true solution. This confirms the observation that in such cases, if the term (noise term) appears, the K^{th} solution will equal the real solution.

5. Conclusion

The conclusion highlights the effectiveness of the numerical approach in solving differential equations with fractional orders, particularly in facilitating the solution process. It emphasizes that in certain cases, such as the last example in the paper, the method enables the discovery of the true solution after only a few steps. The phenomenon where intermediate terms disappear during addition operations confirms the attainment of exact solutions. Additionally, the conclusion underscores the agreement between approximate solutions and real solutions, especially when the fractional derivatives approach the correct values.

This study contributes to the advancement of the field by showcasing the efficacy of numerical methods in handling fractional differential equations. It provides a clear scientific justification for the work by demonstrating its ability to yield accurate solutions efficiently. Furthermore, the potential applications of this method in various fields where fractional differential equations arise can be significant. Extensions of this work could involve exploring more complex differential equations or applying the method to practical problems in physics, engineering, or other scientific disciplines.

FUNDING

None

ACKNOWLEDGEMENT

We are grateful to University of Technology- Iraq, Mustansiriyah University and Universite d'Angers for providing support to accomplish this work.

CONFLICTS OF INTEREST

The authors declare no conflict of interest

REFERENCES

[1] A. A. Gaber, A. F. Aljohani, A. Ebaid, and J. Tenreiro Machado, "The generalized Kudryashov method for nonlinear space–time fractional partial differential equations of Burgers type," Nonlinear Dynamics, vol. 95, no. 1, pp. 361–368, Sep. 2018, doi: https://doi.org/10.1007/s11071-018-4568-4.

[2] B. Zhu, L. Liu, and Y. Wu, "Existence and uniqueness of global mild solutions for a class of nonlinear fractional reaction–diffusion equations with delay," Computers & Mathematics with Applications, vol. 78, no. 6, pp. 1811–1818, Sep. 2019, doi: https://doi.org/10.1016/j.camwa.2016.01.028.

[3] Behrouz Parsa Moghaddam, A. Tenreiro, and M. L. Morgado, "Numerical approach for a class of distributed order time fractional partial differential equations," vol. 136, pp. 152–162, Feb. 2019, doi: https://doi.org/10.1016/j.apnum.2018.09.019.

[4] D. Ziane, D. Baleanu, K. Belghaba, and M. Hamdi Cherif, "Local fractional Sumudu decomposition method for linear partial differential equations with local fractional derivative," Journal of King Saud University - Science, vol. 31, no. 1, pp. 83–88, Jan. 2019, doi: https://doi.org/10.1016/j.jksus.2017.05.002.

[5] R. I. Nuruddeen, "Elzaki Decomposition Method and its Applications in Solving Linear and Nonlinear Schrodinger Equations," Sohag Journal of Mathematics, vol. 4, no. 2, pp. 31–35, May 2017, doi: https://doi.org/10.18576/sjm/040201.

[6] L.-D. Guo, S.-J. Huang, and L.-B. Wu, "Novel Delay-Decomposing Approaches to Absolute Stability Criteria for Neutral-Type Lur'e Systems," Mathematical Problems in Engineering, vol. 2019, pp. 1–10, Dec. 2019, doi: https://doi.org/10.1155/2019/4969470.

[7] B. B. Mandelbrot and J. W. Van Ness, "Fractional Brownian Motions, Fractional Noises and Applications," SIAM Review, vol. 10, no. 4, pp. 422–437, Oct. 1968, doi: https://doi.org/10.1137/1010093.

[8] J.-S. .R. Jang, "ANFIS: adaptive-network-based fuzzy inference system," IEEE Transactions on Systems, Man, and Cybernetics, vol. 23, no. 3, pp. 665–685, 1993, doi: https://doi.org/10.1109/21.256541.

[9] R. Shah, H. Khan, Poom Kumam, M. Arif, and Dumitru Baleanu, "Natural Transform Decomposition Method for Solving Fractional-Order Partial Differential Equations with Proportional Delay," vol. 7, no. 6, pp. 532–532, Jun. 2019, doi: https://doi.org/10.3390/math7060532.

[10] K. Maleknejad, H. Mohammadikia, and J. Rashidinia, "A numerical method for solving a system of Volterra–Fredholm integral equations of the second kind based on the meshless method," Afrika Matematika, vol. 29, no. 5–6, pp. 955–965, May 2018, doi: https://doi.org/10.1007/s13370-018-0589-x.

[11] S. Sh. Ahmed, S. A. H. Salih, and M. R. Ahmed, "Laplace Adomian and Laplace Modified Adomian Decomposition Methods for Solving Nonlinear Integro-Fractional Differential Equations of the Volterra-Hammerstein Type," Iraqi Journal of Science, pp. 2207–2222, Oct. 2019, doi: https://doi.org/10.24996/ijs.2019.60.10.15.

[12] R. Amin, K. Shah, M. Asif, I. Khan, and F. Ullah, "An efficient algorithm for numerical solution of fractional integro-differential equations via Haar wavelet," Journal of Computational and Applied Mathematics, vol. 381, pp. 113028–113028, Jan. 2021, doi: https://doi.org/10.1016/j.cam.2020.113028.

[13] M. Raissi and G. E. Karniadakis, "Hidden physics models: Machine learning of nonlinear partial differential equations," Journal of Computational Physics, vol. 357, pp. 125–141, Mar. 2018, doi: https://doi.org/10.1016/j.jcp.2017.11.039.

[14] H. Durur, O. Tasbozan, and A. Kurt, "New Analytical Solutions of Conformable Time Fractional Bad and Good Modified Boussinesq Equations," Applied Mathematics and Nonlinear Sciences, vol. 5, no. 1, pp. 447–454, Jan. 2020, doi: https://doi.org/10.2478/amns.2020.1.00042.

[15] H. Fu and H. Wang, "A Preconditioned Fast Parareal Finite Difference Method for Space-Time Fractional Partial Differential Equation," vol. 78, no. 3, pp. 1724–1743, Sep. 2018, doi: https://doi.org/10.1007/s10915-018-0835-2.

[16] Weinan E, M. Hutzenthaler, A. Jentzen, and T. Kruse, "On Multilevel Picard Numerical Approximations for High-Dimensional Nonlinear Parabolic Partial Differential Equations and High-Dimensional Nonlinear Backward Stochastic Differential Equations," Journal of Scientific Computing, vol. 79, no. 3, pp. 1534–1571, Aug. 2017, doi: https://doi.org/10.1007/s10915-018-00903-0.

[17] A. A. Gaber, A. F. Aljohani, A. Ebaid, and J. Tenreiro Machado, "The generalized Kudryashov method for nonlinear space–time fractional partial differential equations of Burgers type," Nonlinear Dynamics, vol. 95, no. 1, pp. 361–368, Sep. 2018, doi: https://doi.org/10.1007/s11071-018-4568-4.

[18] H. Jafari and S. Seifi, "Solving a system of nonlinear fractional partial differential equations using homotopy analysis method," Communications in Nonlinear Science and Numerical Simulation, vol. 14, no. 5, pp. 1962–1969, May 2009, doi: https://doi.org/10.1016/j.cnsns.2008.06.019.

[19] L. Aceto, D. Bertaccini, Fabio Durastante, and Paolo Novati, "Rational Krylov methods for functions of matrices with applications to fractional partial differential equations," Journal of Computational Physics, vol. 396, pp. 470–482, Nov. 2019, doi: https://doi.org/10.1016/j.jcp.2019.07.009.

[20] B. Zhu, L. Liu, and Y. Wu, "Existence and uniqueness of global mild solutions for a class of nonlinear fractional reaction–diffusion equations with delay," Computers & Mathematics with Applications, vol. 78, no. 6, pp. 1811–1818, Sep. 2019, doi: https://doi.org/10.1016/j.camwa.2016.01.028.

[21] Behrouz Parsa Moghaddam, A. Tenreiro, and M. L. Morgado, "Numerical approach for a class of distributed order time fractional partial differential equations," vol. 136, pp. 152–162, Feb. 2019, doi: https://doi.org/10.1016/j.apnum.2018.09.019.

[22] S. Biswas, S. Moi, and Smita Pal Sarkar, "Neutrosophic Riemann integration and its properties," *Soft computing*, vol. 25, no. 22, pp. 13987–13999, Sep. 2021, doi: https://doi.org/10.1007/s00500-021-06200-7.

[23] Segun, Akerele Olofin, "Riemann Integration in the Euclidean Space," *arXiv (Cornell University)*, Mar. 2024, doi: https://doi.org/10.48550/arxiv.2403.19703.

[24] S. Axler, "Riemann Integration," *Graduate texts in mathematics*, pp. 1–12, Nov. 2019, doi: https://doi.org/10.1007/978-3-030-33143-6_1.

[25] C. Wang and R. P. Agarwal, "Riemann Integration, Stochastic Calculus, and Shift Operators on Time Scales," *Developments in mathematics*, pp. 1–115, Jan. 2022, doi: https://doi.org/10.1007/978-3-031-11619-3_1.

[26] D. E. Betancur-Herrera and N. Muñoz-Galeano, "A numerical method for solving Caputo's and Riemann-Liouville's fractional differential equations which includes multi-order fractional derivatives and variable coefficients," *Communications in Nonlinear Science and Numerical Simulation*, vol. 84, p. 105180, May 2020, doi: https://doi.org/10.1016/j.cnsns.2020.105180.

[27] D. Santina, N. Kamran, M. Asif, Salma Aljawi, and Nabil Mlaiki, "Application of the inverse Laplace transform techniques to solve the generalized Bagley–Torvik equation including Caputo's fractional derivative," *Partial differential equations in applied mathematics*, vol. 10, pp. 100664–100664, Jun. 2024, doi: https://doi.org/10.1016/j.padiff.2024.100664.

[28] M. Rafiq *et al.*, "Series solution to fractional contact problem using Caputo's derivative," *Open Physics*, vol. 19, no. 1, pp. 402–412, Jan. 2021, doi: https://doi.org/10.1515/phys-2021-0046.

[29] Hassen Arfaoui, "Polynomial decay of a linear system of PDEs via Caputo fractional-time derivative," *Mathematical methods in the applied sciences*, Apr. 2024, doi: https://doi.org/10.1002/mma.10135.

[30] Humberto, R. Dantas, Filipe, and Davidson Martins Moreira, "Three-Dimensional Analytical Solution of the Fractional Atmospheric Pollutant Dispersion Equation Considering Caputo and Conformable Derivatives," *Pure and Applied Geophysics*, vol. 179, no. 9, pp. 3411–3426, Aug. 2022, doi: https://doi.org/10.1007/s00024-022-03114-9.